IEEE Access
Multidisciplinary | Rapid Review | Open Access Journal

Received April 5, 2022, accepted May 12, 2022, date of publication May 16, 2022, date of current version May 25, 2022.

Digital Object Identifier 10.1109/ACCESS.2022.3175567

Utilization of Galvanic Couples in Wireless Network for Salinity Deposition Sensing

NORIKAZU FUSE[1], (Member, IEEE), MAO TAKEYAMA[2], MASAHITO MIYOSHI[1], NAOTO KIHARA[2], YOSHIHARU SHUMUTA[2], YASUHIKO HORI[1], AND JUN-ICHI TANI[3]

[1]Grid Innovation Research Laboratory, Central Research Institute of Electric Power Industry, Yokosuka 240-0196, Japan
[2]Sustainable System Research Laboratory, Central Research Institute of Electric Power Industry, Abiko 270-1194, Japan
[3]Energy Transformation Research Laboratory, Central Research Institute of Electric Power Industry, Yokosuka 240-0196, Japan

Corresponding author: Norikazu Fuse (fuse@criepi.denken.or.jp)

ABSTRACT Galvanic couples traditionally used for the evaluation of atmospheric corrosivity are constant monitoring sensors whose output correlates with the deposition of sea salt. This report provides the conversion methodology needed to monitor real-time airborne salinity. The methodology was validated by wireless observations made in two Japanese coastal areas, where a remarkable increase in salt deposition revealed rapid contamination. Additionally, the amount of deposition varied according to distance from the shore. Solar radiation reduced the sensor output and induced a sharp drop in the estimated deposition. These unexpected discrepancies were resolved by considering surface humidity, which was reduced by surface heating.

INDEX TERMS Galvanic couples, data analysis, wireless network, sea-salt deposition, rapid contamination, surface humidity, solar radiation.

I. INTRODUCTION

Monitoring the air-borne salinity and its deposition is important for insulators because deliquescence could reduce the insulation strength of electrical equipment. This need becomes stronger when storms are approaching and so-called rapid contamination is concerned. The galvanic couples developed to evaluate the corrosion environment are a promising tool for this purpose because they are designed to perform constant monitoring and to withstand being exposed outdoors [1]–[3]. As the sensor outputs are determined by the combination of the amount of sea salt deposition (W_S) and humidity, their back calculation enables to estimate W_S values from the sensor observation [4]–[6]. That is to say, the overall framework of the study is to estimate W_S values from the simultaneous measurements of humidity and galvanic sensing. The specific progress made herein is the establishment of data correlation methodology that is required to deal with field data. Its utility was validated for the field data obtained in two Japanese coastal areas.

A specific feature of a galvanic couple is its wireless measurement record over a year [7]. The robustness and passive measurement features of the galvanic couple are attractive for this type of measurement in the field. Wireless networking enables users to monitor the real-time situation through the data server, and also provide the latest analysis technology even during the period of observation.

To the authors' knowledge, no traditional technique has realized real-time sensing for salinity in the gas phase. Traditional techniques usually require large and expensive systems and/or chemical laboratory analyses. For example, gauzes are used in an international standard to collect the salinity [8]. This is not a real-time monitoring because at least for a month of field exposure and time-consuming laboratory analysis such as titration or ion chromatography are required. A dummy insulator is installed in some Japanese substations to evaluate its W_S [9]–[12]. However, literature pointed out that the data reliability would be eroded if the measurement is conducted frequently [10]; the dummy must be removed from the area and transferred to a steam chamber for the measurement. Recently, potentiometric chloride sensors adoptable for wireless sensing were reported to evaluate the salinity in soil [13], [14]. Its sensing postulates that redox reaction in soil phase takes place similar to the case in aqueous media.

II. PRINCIPLE OF THE ANALYSIS

The sensor used is a stripe-patterned layered Zn–Ag galvanic couple with an insulation sheet. Its output current is governed

The associate editor coordinating the review of this manuscript and approving it for publication was Binit Lukose.

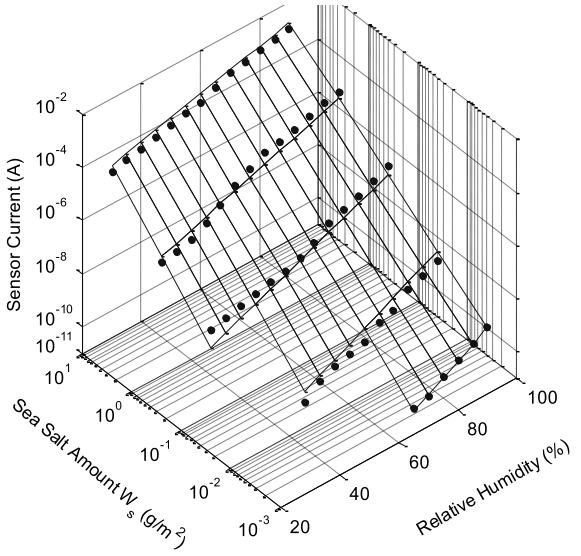

FIGURE 1. Output characteristics of Zn-Ag-type ACM sensor as a function of sea salt amount and humidity [3]. Approximated surface constructed in [4]–[6] was used in the analysis.

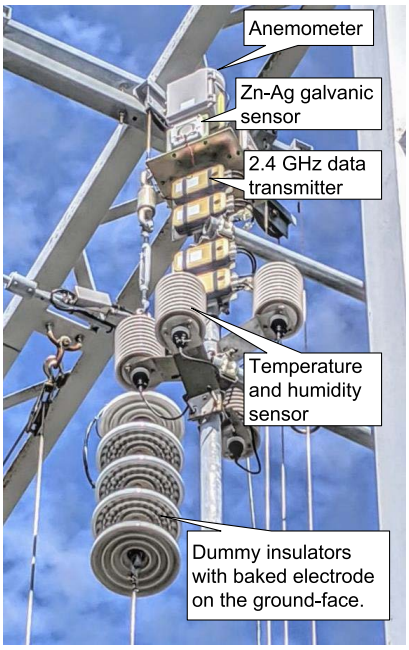

FIGURE 2. Example of an observation setup in the Sagami Bay area. Five series of dummy insulators next to the sensors were used to measure their surface conductivity.

by the wetness of the sensor surface, which is determined by W_S and relative humidity. Three-dimensional representation of such characteristic is depicted in Fig. 1 [3]. The W_S value can be estimated by inserting the observed data set of the sensor output and humidity into this three-dimensional sensor characteristic. The present study estimated W_S for all instantaneous data observed every 10 minutes, which contain outlier outputs that needed to be corrected.

The first outlier is raid surge typically observed in the rainfall period [3]. Its large value leads to an overestimation of the W_S value. This study extracted these outliers using the automated judgment algorithm established previously by other authors [4]–[6]. The extracted outliers were multiplied by a correlation factor of 0.2 that was established for corrosion rate estimation [3].

Another outlier is the output affected by solar radiation. A preceding study reported that the output of a wetness sensor was reduced when the sensor was exposed to the sun in order to increase the surface temperature T_S and reduce the surface humidity ϕ_S [15]. The present study then calculated saturated vapor pressure from the atmospheric temperature and humidly (T_A and ϕ_A) to estimate ϕ_S, based on the T_S measurement.

III. EXPERIMENTAL PROCEDURES

The observation was initiated in February 2021. Two Japanese coastal areas, facing the Sagami and Sasebo bays, were selected as observation areas. The selection process of the observation area is described in the Appendix. The Zn–Ag couple sensor was manufactured in accordance with an industrial standard [16]. An example of the observation scene is depicted in Fig. 2. All sensors were oriented to face the south. Wireless 2.4 GHz local networks were established

TABLE 1. Main features of salinity evaluation methods used.

Method	Real-time operatability		Margin of data error	Areas applied
	Data interval	Elapsed time		
Galvanic sensing	10 min.	~30 ms [6]	−55% - +120% [4], [5]	Sagami and Sasebo areas
Insulator's resistivity	8 hours	~20 min.	−32% - +32% [a]	Sagami area only
Meteoro-logical calculation	10 min.	110 min. [b]	−50% - +50% [c]	Sagami area only

[a] Data scattering reported in [9].
[b] Calculator used: HPE SGI 8600 with Intel Xeon Gold 6148 processor. Meteorological record was used to trace the typhoon path.
[c] Data scattering reported in [17].

in each area to store the obtained data on the web server. The Sagami area, located in Yokosuka City, additionally measured solar radiation using a pyranometer, and T_S using the T-type thermocouple. Salinity deposited on a dummy ceramic insulator was estimated from the surface conductivity of a dummy insulator—a traditional evaluation method in the electric industry [9]. The airborne salinity at the area was also numerically calculated based on the WRF model [17], [18]. The main features of these methods are compared in Table 1; the areas where the methods were applied are included. The dummy measurement was conducted every eight hours to avoid the uncertainty pointed out in [10]. The numerical calculation used the meteorological record, since prediction of typhoon path is a challenging task. These two methods were only applied for the Sagami area. The Transmission

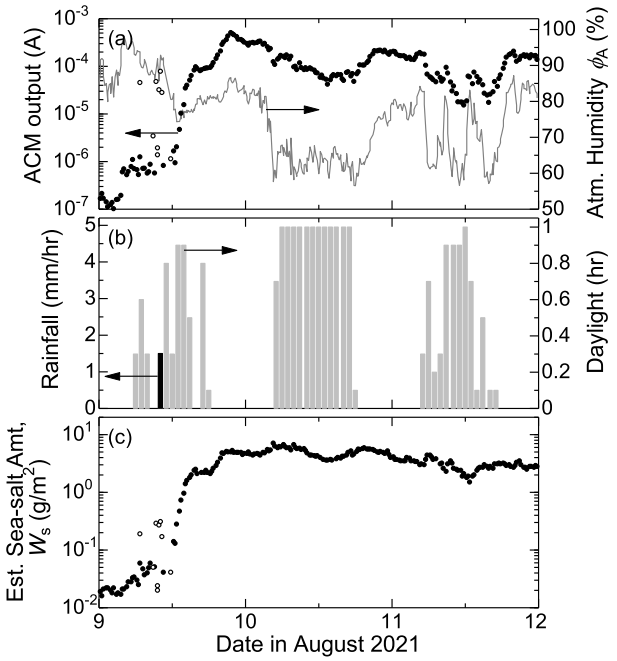

FIGURE 3. (a) Temporal changes in galvanic outputs and atmospheric humidity observed in the Sagami Bay area in August 2021. The outputs are represented by dotted symbols and the outliers are represented by open symbols. Such data sets are converted to sea salt amount W_S in (c) with the same notations. (b) Daylight duration and rainfall measured every hour at the nearest meteorological observatory. The daylight duration is defined as the time when the direct solar irradiance exceeds 120 W/m^2.

towers were used for performing observation in the Sasebo area.

IV. RESULTS AND DISCUSSION

Rapid increases in galvanic current outputs from sub-μA to sub-mA were observed at the sensor installed in the Sagami coastal area when typhoon Miriane approached in August 2021 (Fig. 3). Records of the nearest meteorological observatory [19] show only slight rains because the typhoon did not hit the observation area itself. Instantaneous sensor outputs only observed in this rainy period were judged to be outliers, to prove that the automated judgment algorithm worked normally. Such data were coupled with the corresponding ϕ_A value to convert into W_s by plugging them into the sensor's characteristic. The obtained W_s value showed a sudden surge from 0.01 to 1 g/m^2 and a gradual decrease for approximately 10 days thereafter.

These temporal changes in salinity were compared to the one estimated from the dummy insulator in Fig. 4. This figure also shows the calculated airborne salinity. The three trends agreed with each other, suggesting the plausibility of the analyses. What is important herein is the fact that real-time value is only obtained from the galvanic output.

According to a chemical analysis conducted for sensors removed from the field, the error range was found to be $10^{\pm 0.35}$ against the estimated value for W_s determined by the sensor output [4], [5]. Milder temporal changes were evaluated for the dummy than the ones from the galvanic sensor

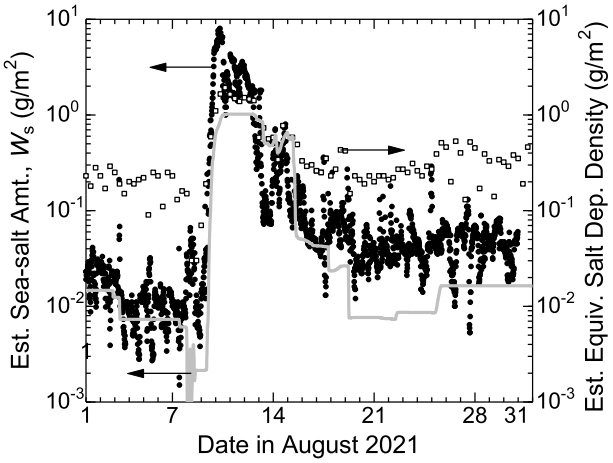

FIGURE 4. Comparison of the temporal changes in salinity estimated for the Sagami Bay area in August 2021. Solid circles indicate W_S values estimated from the galvanic output. Open squares indicate equivalent salt-deposition density, estimated from the surface conductivity of the dummy insulator. Gray curves indicate the result of W_S calculation obtained by taking the climatic physical processes into account.

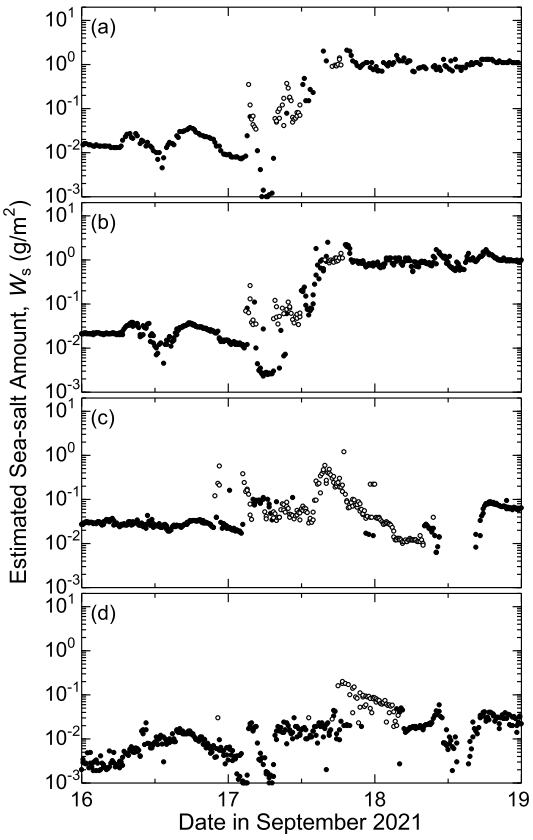

FIGURE 5. Temporal changes in estimated depoaread sea salt amount, based on galvanic output observed for towers in the Sasebo area at distances of 0.9 km (a), 1.6 km (b), 3.6 km (c), and 5.0 km (d) from the shore. The designations of the symbols are the same as in Fig. 3 (a).

in Fig. 4. This may be attributed to the orientation of the measurement surface: the insulator's ground-facing surface was used for the dummy measurement; whereas the galvanic

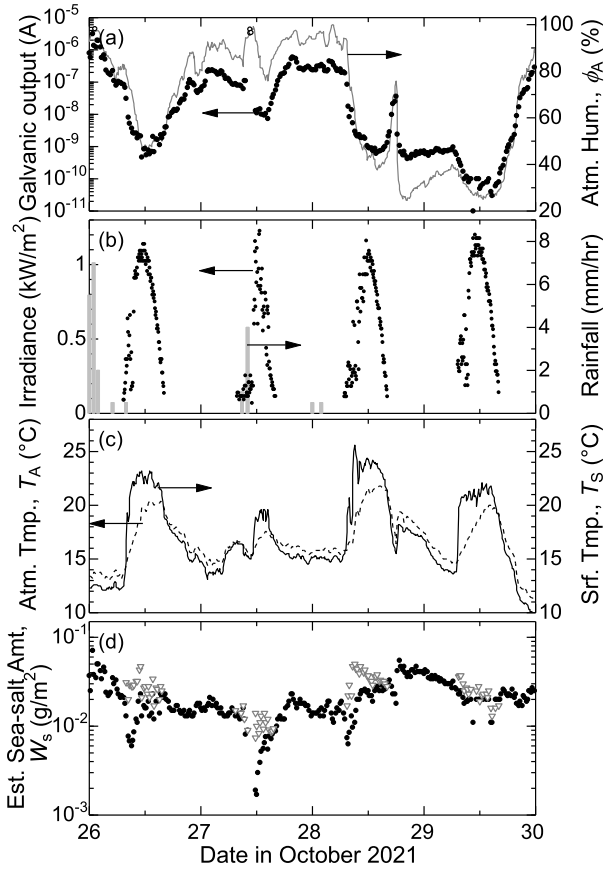

FIGURE 6. **(a) Temporal changes in galvanic outputs and atmospheric humidity observed at the Sagami area in October 2021. The designations of the symbols are the same as in Fig. 3 (a). (b) Solar irradiance measured at the area, as well as the daylight duration measured at the nearest observatory. (c) The changes in atmospheric and surface temperature. The sea salt amount W_s estimated with and without correlation of the solar effect is respectively represented by open triangles and solid circles in (d).**

sensor was always directly exposed to rain, wind, and sun. Equivalent salt-deposition density is adopted for the salinity value in the dummy insulator to meet the standard [20]. This was calculated by adapting the measured surface conductivity in wet conditions to the conduction characteristic of NaCl, which is expressed as $\rho_{\mathrm{NaCl}} = 6.2 \times \sigma^{1.08}$. Here ρ is concentration in g/L and σ is the conductivity in S/m. On the other hand, W_s values estimated from the galvanic sensor are secured by the chemical analyses results [4], [5]. The relationship between the conductivity and ion chromatography results for depoaread matters on sensors removed from the field provided a similar expression: $\rho_{\mathrm{Ws}} = 8.4 \times \sigma^{1.12}$. The two equations are almost identical, allowing the direct comparison of the two vertical axes in Fig. 4.

Similar analysis was also conducted for the sensor outputs observed for transmission towers in the Sasebo area. Fig. 5 shows the typical W_s analysis results obtained when another typhoon, Chanthu, approached the area in September 2021. The results obtained at that time confirmed distance dependence. That is, the W_s value during the typhoon decreased by one tenth when changing the distance from 1.6 to 5.0 km. Another interesting finding was the fact that the W_s value obtained for normal sensor output and for outlier output showed continuous temporal changes. This result is considered to bring a certain degree of validity to the data correction for outliers related to rainfall. Note that data correction for solar radiation effect was not conducted for the above-mentioned results, since T_S measurement was not performed.

Fig. 6 shows an example of the correction against solar radiation effect, for the data observed in the Sagami area, where the T_S measurement was performed. The sensor output showed a decrease during the daylight period. A remarkable feature was observed on October 27th when the sensor output suddenly decreased after the rainfall stopped and T_S was raised. The W_s obtained without the correction also showed a reduction by one twentieth to emerge rapid dip. To resolve the dip, the correction was performed by using ϕ_S instead of ϕ_A to obtain W_s, for data observed when T_S was higher than T_A. The average wind speed was 4 m/s during the period in Fig. 6 and no strong winds were observed. Therefore, corrected W_s changes are preferable from the perspective of climatic phenomenon. Data scattering still remained in the corrected W_s trend, but the direction of sophistication in analysis was confirmed from the figure.

V. CONCLUSION

Galvanic couples traditionally used for corrosion sensors were taken on a subject for salt-deposition meter for their ability of continuous monitoring. Wireless field measurements in two Japanese coastal areas facing the Sagami and Sasebo bays validated its utility at least for the analysis of rapid contamination. That is, rapid increases in galvanic current outputs observed when a typhoon approached were successfully converted to the amount of sea salt-deposition to show a surge from about 0.01 to 1 g/m^2. The trend of the estimated salinity matched the results obtained using the conventional instrument, as well as the ones obtained for airborne salinity calculations. Solar radiation reduced the sensor output and induced a sharp drop in estimated deposition value. Surface temperature measurement was confirmed to correct such data scattering by calculating the surface humidity.

APPENDIX

This section describes the selection of the observation area. The Sagami Bay area is first selected to realize easy access and maintenance activities because the area is located in our yard. Contrary, the observation in transmission towers was to confirm how the sensor works in an environment where salinity decreases according to the distance from the shore. Five Japanese coastal areas were subjected to assess their applicability under the view of annual salinity (Table 2) using the fluid dynamics model [21], [22]. Corrosion severity was also evaluated according to the ISO standard [23] because it affects the maintenance frequency of the sensor. The assessed results were as follows:

TABLE 2. Assessment results of salinity and corrosivity to determine the observation area.

Area code	Ocean facing To the area	Assessment Item	Distance from shore		
			~0.4 km	~4.5 km	~7.5 km
A	Local bay	Annu. Avg. Cl^- [mg/(m^2·day)] [a]	126	76	58
		Corrosion rate [μm/year] [b]	44	39	37
		Category [b]	C3	C3	C3
B	East China Sea	Annu. Avg. Cl^- [mg/(m^2·day)] [a]	217	83	-
		Corrosion rate [μm/year] [b]	61	42	-
		Category [b]	C4	C3	-
C	East China Sea	Annu. Avg. Cl^- [mg/(m^2·day)] [a]	90	69	57
		Corrosion rate [μm/year] [b]	39	37	33
		Category [b]	C3	C3	C3
D	Pacific Ocean	Annu. Avg. Cl^- [mg/(m^2·day)] [a]	77	57	41
		Corrosion rate [μm/year] [b]	31	29	29
		Category [b]	C3	C3	C3
E	Pacific Ocean	Annu. Avg. Cl^- [mg/(m^2·day)] [a]	64	50	44
		Corrosion rate [μm/year] [b]	28	31	31
		Category [b]	C3	C3	C3

[a] Numerical calculation results obtained by the fluid dynamics model [20], [21]
[b] Calculated for carbon steels according to ISO 9223 [22].
[c] Corrosive severity according to ISO 9223 [22].

- Area A: Significant change in salinity was expected to show the distance dependence. Concern has been raised that the knowledge gained could be limited because the area faces a local bay.
- Area B: The most significant change in salinity and resultant distance dependence from the shore was expected. Long-distance dependence cannot be evaluated because the area is located on a peninsula. Frequent maintenance was required because of the severe corrosion environment.
- Area C: Significant change in salinity was expected to show the distance dependence. The appropriate corrosion severity predicted that the galvanic sensor works normally. This is the Sasebo area that finally passed the assessment.
- Area D: Corrosion severity was expected to be appropriate, but milder than Area C. The distance dependence of salinity was also expected to be mild. The advantages of Area C were highlighted.
- Area E: Very mild decrease in salinity is expected along with the distance from the shore.

ACKNOWLEDGMENT

The authors would like to express their sincere thanks to the electric power utility company who provided the area for on-area observation for their intensive technical supports.

REFERENCES

[1] F. Mansfeld and J. V. Kenkel, "Electrochemical monitoring of atmospheric corrosion phenomena," *Corrosion Sci.*, vol. 16, no. 3, pp. 111–112, 1976.
[2] N. D. Tomashov, *Theory of Corrosion and Protection of Metals*. New York, NY, USA: MacMillan, 1966.
[3] T. Shinohara, "Evaluation and monitoring methods for atmospheric corrosion," *Zairyo-Kankyo*, vol. 64, no. 2, pp. 26–33, 2015.
[4] N. Fuse, A. Naganuma, T. Fukuchi, J.-I. Tani, and Y. Hori, "Methodology to improve corrosion rate estimation based on atmospheric corrosion monitoring sensors," *Corrosion*, vol. 73, no. 2, pp. 199–209, Feb. 2017.
[5] N. Fuse, Y. Shumuta, A. Naganuma, J.-I. Tani, and Y. Hori, "Corrosion rate estimation based on sensor monitoring: Field test validation in transmission towers," *Corrosion*, vol. 75, no. 7, pp. 839–847, Jul. 2019.
[6] N. Fuse, A. Naganuma, Y. Shumuta, J.-I. Tani, and Y. Hori, "Development of quantitative analytical program for corrosion sensor data," *Zairyo-Kankyo*, vol. 70, no. 2, pp. 47–54, 2021.
[7] Y. Shumuta, H. Fukutomi, Y. Hori, and K. Ishizawa, "Observation of corrosion environment in transmission towers—Part 3: Development of a wireless corrosion environment monitoring system," in *Proc. Annu. Conf. IEEJ Power Energy Soc.*, Tokushima, Japan, 2018, pp. 9-6-9–9-6-10.
[8] *Corrosion of Metals and Alloys—Corrosivity of Atmospheres—Measurement of Environmental Parameters Affecting Corrosivity of Atmospheres*, Standard 9225, 2012.
[9] M. Yamamoto and S. Sogabe, "Tests on contamination measurement by means of 'saltmeter'—Insulator contamination detector," in *Proc. CIGRE SC 33 Colloq.*, Tokyo, Japan, 1987.
[10] M. Nakamura, W. Huang, S. Goto, and T. Taniguchi, "Determination of timing for measurement and washing of polluted insulators in substations," *IEEJ Trans. Power Energy*, vol. 122, no. 2, pp. 314–322, 2002.
[11] H. Suto, Y. Hattori, H. Hirakuchi, T. Ishikawa, T. Takahashi, S. Utsunomiya, and H. Moritaka, "Estimation of insulator pollution during a typhoon using a numerical simulation of wind and sea-salt particle transport," in *Proc. IEEJ Tech. Meet. High Voltage Eng.*, 2009.
[12] T. Kuroyagi and K. Fujiwara, "Charactoristics of salt contamination and withstand voltage of polmer insulators for transmission lines," Central Res. Inst. Electr. Power Ind., Yokosuka, Res. Rep. H08018, 2009. [Online]. Available: https://criepi.denken.or.jp/hokokusho/pb/reportDetail?reportNoUkCode=H08018
[13] A. Cranny, N. R. Harris, M. Nie, J. A. Wharton, R. J. K. Wood, and K. R. Stokes, "Screen-printed potentiometric Ag/AgCl chloride sensors: Lifetime performance and their use in soil salt measurements," *Sens. Actuators A, Phys.*, vol. 169, no. 2, pp. 288–294, Oct. 2011.
[14] N. Harris, A. Cranny, M. Rivers, K. Smettem, and E. G. Barrett-Lennard, "Application of distributed wireless chloride sensors to environmental monitoring: Initial results," *IEEE Trans. Instrum. Meas.*, vol. 65, no. 4, pp. 736–743, Apr. 2016.
[15] M. Hoseinpoor, T. Prošek, L. Babusiaux, and J. Mallégol, "Toward more realistic time of wetness measurement by means of surface relative humidity," *Corrosion Sci.*, vol. 177, Dec. 2020, Art. no. 108999.
[16] *Atmospheric Corrosion Monitoring Sensor*, Jpn. Ind. Standard JIS Z 2384, 2019.
[17] N. Kihara, H. Hirakuchi, A. Takahashi, S. Ohara, and S. Fujita, "Numerical study on seasalt depositions in Niigata prefecture, Japan," in *Proc. 7th Asian Aerosol Conf.*, 2011, pp. 635–640.

[18] Y. Shumuta, N. Kihara, Y. Hattori, H. Suto, H. Hirakuchi, M. Ishida, J. Takemura, and K. Nakazumi, "Sensitivity analysis for estimating salt-induced damage to voltage-current transformers due to typhoons," *Electr. Eng. Jpn.*, vol. 193, no. 3, pp. 34–43, Nov. 2015.
[19] Japan Meteorological Agency. *Kakono Kisyo Deta Kensaku (Past Meteorological Data Search)*. Accessed: Feb. 1, 2022. [Online]. Available: https://www.data.jma.go.jp/obd/stats/etrn/
[20] *High-Voltage Testing Techniques*, IEEE Standard 4, 2013.
[21] H. Suto, Y. Hattori, N. Tanaka, and Y. Kohno, "Effects of strong wind and ozone on localized tree decline in the Tanzawa mountains of Japan," *Asian J. Atmos. Environ.*, vol. 2, no. 2, pp. 81–89, Dec. 2008.
[22] R. Onishi, K. Matsuda, H. Suto, Y. Hattori, H. Hirakuchi, S. Matsunami, S. Yagyu, T. Shinohara, and H. Katayama, "High-resolution prediction for the amount of airborne sea salt by multi-scale weather simulation," *Mater. Trans.*, vol. 62, no. 12, pp. 1785–1790, 2021.
[23] *Corrosion of Metals and Alloys—Corrosivity of Atmospheres—Classification, Determination and Estimation*, Standard 9223, ISO, Geneva, Switzerland, 2012.

NORIKAZU FUSE (Member, IEEE) was born in Tokyo, Japan, in April 1980. He received the B.Eng., M.Eng., and Dr.Eng. degrees from Waseda University, in 2003, 2005, and 2009, respectively. He was a Research Fellow with the Japan Society for the Promotion of Science, from 2005 to 2008, and a Research Associate with Waseda University, from 2008 to 2010. He is currently a Research Scientist with the Central Research Institute of Electric Power Industry (CRIEPI). He was commended by the Institute of Electric Engineers Japan (IEEJ) for the Distinguished Paper Awards, in 2013 and 2019.

MAO TAKEYAMA was born in Japan, in 1993. He received the B.S. degree from the Faculty of Engineering, Kyoto University, Japan, in 2017, and the Ph.D. degree from the Department of Nuclear Engineering, Kyoto University, in 2020. He is currently working with CRIEPI. His major research interest includes multiphase flow.

MASAHITO MIYOSHI was born in Kanagawa, Japan, in July 1993. He received the B.E. and M.E. degrees in mechanical systems engineering from Tokyo City University, in 2016 and 2018, respectively. In 2018, he joined CRIEPI. His research interests include high voltage phenomena and outdoor insulators.

NAOTO KIHARA received the Ph.D. degree in earth and planetary sciences from Kyoto University, Japan, in 2006. He is currently a Senior Researcher with CRIEPI. He is an expert of air-sea interactions, including sea salt/spray emissions and transport and tsunami engineering. He is a member of the Japan Society of Civil Engineers (JSCE), the Japan Society of Mechanical Engineers, and the Japan Association for Earthquake Engineering.

YOSHIHARU SHUMUTA joined CRIEPI, in 1991. His research area is reliability engineering and risk management, with a focus on emergency response issues against natural disaster and maintenance technologies using IoT for electric power lifeline systems. It covers electric power civil engineering structures and transmission and distribution equipment. He concurrently serves as a Professor in Kanagawa University since 2022. He won the OHM Technology Award of the Promotion Foundation for Electric Science and Engineering, in 2010; the IEEJ Distinguished Paper Award, in 2011; the Sibusawa Award, in 2012; and the Japan Society of Corrosion Engineering (JSCE) Award, in 2021. He is a member of JSCE and IEEJ.

YASUHIKO HORI received the M.Eng. and Dr.Eng. degrees from Tsukuba University, in 1989 and 1991, respectively. He is currently a Senior Researcher with CRIEPI. His research interest includes thermal analysis for diagnosis of electric and power apparatus.

JUN-ICHI TANI received the M.Eng. and Dr.Eng. degrees from Tohoku University, in 1992 and 2006, respectively. He is currently a Senior Researcher with CRIEPI. He is also a Board Member of JSCE.